BNL 65605

Results of Stretched Wire Field Integral Measurements on the Mini-Undulator Magnet –

Comparison of Results Obtained from Circular and Translational Motion of the Integrating Wire

Lorraine Solomon
Brookhaven National Laboratory
Upton, New York, USA

April 1998

National Synchrotron Light Source

Brookhaven National Laboratory
Operated by
Brookhaven Science Associates
Upton, NY 11973

Under Contract with the United States Department of Energy
Contract Number DE-AC02-98CH10886

DISCLAIMER

Results of Stretched Wire Field Integral Measurements on the Mini-Undulator Magnet –

Comparison of Results Obtained from Circular and Translational Motion of the Integrating Wire

Lorraine Solomon
April 1998
BNL-NSLS

Measurements of the multipole content of the Mini-Undulator magnet have been made with two different integrating wire techniques. Both measurements used 43 strand Litz wire stretched along the length of the magnet within the magnet gap. In the first technique, the wire motion was purely translational, while in the second technique the wire was moved along a circular path. The induced voltage in the Litz wire was input into a Walker integrator, and the integrator output was analyzed as a function of wire position for determination of the multipole content of the magnetic field.

The mini-undulator magnet is a 10 period, 80 mm per period hybrid insertion device. For all the data contained herein the magnet gap was set at 49 mm. In the mini-undulator magnet, the iron poles are 18mm x 32mm x 86mm, and the Samarium Cobalt permanent magnet blocks are 22mm x 21mm x 110mm. For this magnet, which is a shortened prototype for the NSLS Soft X-Ray Undulator Magnet, the undulator parameter $K = 0.934\, B(\text{Tesla})\lambda(\text{cm})$, and $B(\text{tesla}) = 0.534/\sinh(\pi \text{Gap}/\lambda)$ [1] . At a gap of 49 mm, the magnetic field is 1590 Gauss.

The 43 strand Litz wire is supported on motorized x-y stages at both ends of the magnet, which are controlled by stepping motors through a Labview program. One leg of the wire loop is within the magnet gap, and the other leg is in an essentially field free region. Only the leg of the wire loop within the magnet gap is moved during data acquisition. The Litz wire is tensioned with 11.5 pounds, and is wrapped with a supporting tape which is itself tensioned with 18 pounds through a spring and turnbuckle arrangement. With this setup the sag in the wire over the 72 inch span is less than 0.003 inches, as measured with survey instruments. Photographs of the setup are shown below.

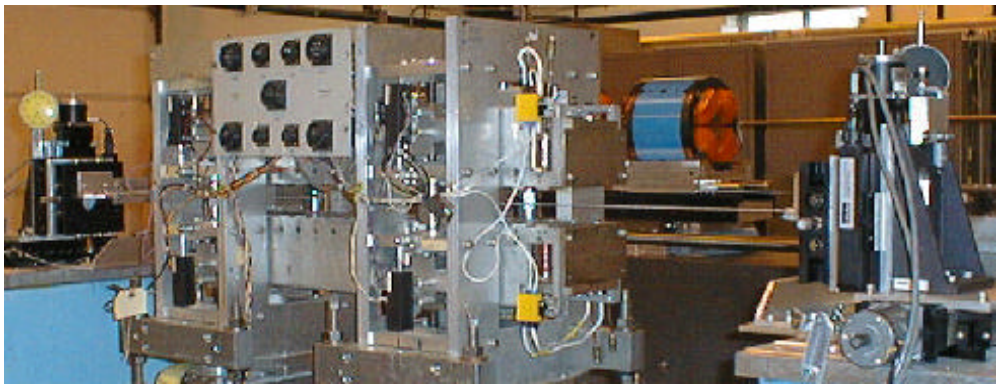

[1] L. Solomon, J. Galayda, and M. Kitamura, Magnetic Measurements of the NSLS Soft X-Ray Undulator. BNL Report 44921

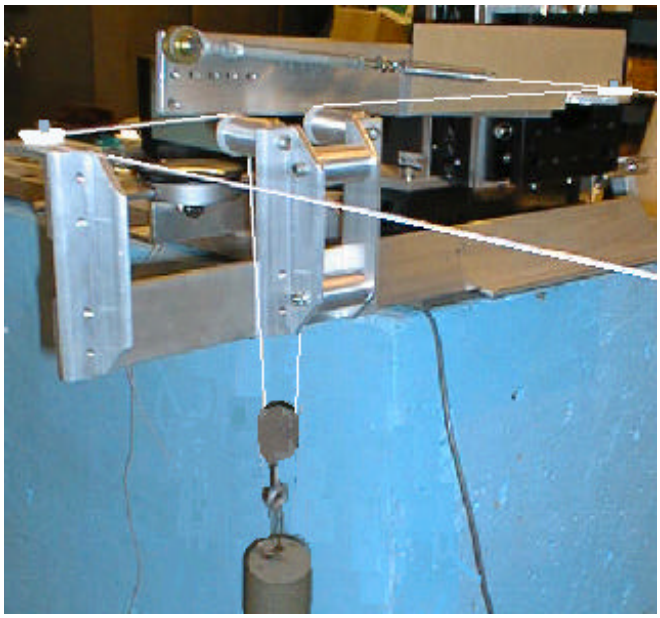

The Litz wire within the magnet gap is moved, and the induced voltage due to the change in the flux intercepted by the coil is input into a Walker integrator. The induced voltage in the coil is related to the change in the magnetic flux enclosed by the coil through the following

$$\int \text{Voltage dt} \ \text{[v-sec]} = N_t * \Delta x \ \text{[m]} * \int B\text{[T]} \ dl\text{[m]} \qquad (1)$$

where N_t is the number of turns in the coil, and Δx is the distance moved by the coil. In the Walker integrator, the front panel reading is

$$\text{Front panel reading} \ [10^{-5} \ T \ m^2] = \frac{\int \text{Voltage dt} \ \text{[v-sec]}}{N \ D} \qquad (2)$$

where N = the thumbwheel setting on the integrator, and D = the decade setting on the integrator.

Combining the two above equations, one gets that

$$\int B \ dl \ \text{[G cm]} = \frac{\text{Front panel reading} * N * D * 10^3}{N_t * \Delta x \ \text{[cm]}} \qquad (3)$$

where Δx is in cm. This form is useful for analysis of translational motion of the Litz wire.

Circular Wire Motion

In the case where the wire motion was circular, the wire was moved along circles with radii 2mm, 7mm, 12mm, 17mm, 20mm, and 24mm. During these scans there were only 34 functioning coil loops within the Litz wire. For these scans, the front panel integrator thumbwheel was set to N = N_t *r[mm] i.e., N= 68, 238, 408, 578, 680, and 816 respectively, and D=10. With these settings, the integrated voltages for the various scans were similar even though the path length through which the wire moved differed (eq. [3]). The wire motion was stopped at 16 points along the circle (i.e. at intervals of 22.5 degrees) and integrator data was obtained. Therefore, the arc length between two adjacent data points varied from 0.8mm to 9.4 mm as the circle radius increased from 2mm to 24 mm, with a concurrent increase in induced wire voltage. Integrator data was taken for motion from a starting wire position to the next wire position, and then also for wire motion back to the starting wire position. The actual integrator signal was taken as half the difference between the two integrator readings, which assumes a linear integrator drift with time. This process was repeated 20 times for each position of the wire, and then averaged to obtain a single data point used in the field analysis. That is, each data point at a given angle is representative of the average of 20 linear drift compensated data points, and 16 data points (i.e. averaged data at 16 angles) are used in the multipole analysis. For this analysis the field is expressed in terms of radial coordinates r and θ, [2]

$$B_r(r,\theta) = \sum [a_n \cos(n\theta) + b_n \sin(n\theta)]\ r^{n-1} \tag{4}$$

$$\int V(r,\theta)\, dt = N_t \int dz \int B_r\, r d\theta \tag{5}$$

where the limits of integration on t are $t_1(\theta_1) \rightarrow t_2(\theta_2)$, on z are $-L/2 \rightarrow L/2$, and on θ are $\theta_1 \rightarrow \theta_2$. Integrating over θ,

$$\int V(r,\theta)\, dt = 2N_t \left\{\sum [A_n \cos(n\theta) - B_n \sin(n\theta)]\right\} \sin(n\Delta\theta/2)\, r^n/n \tag{6}$$

where $A_n = \int a_n\, dz$, $B_n = \int b_n\, dz$, $\Delta\theta = \theta_1 - \theta_2$ and $\theta = \{\theta_1 + \theta_2\}/2$.

Fitting the integrator output to a function of the form

$$\int V\, dt = V_{1,\sin} \sin k\theta + V_{2,\sin} \sin 2k\theta + V_{3,\sin} \sin 3k\theta + V_{1,\cos} \cos k\theta + V_{2,\cos} \cos 2k\theta + V_{3,\cos} \cos 3k\theta \tag{7}$$

where $k = 2\pi/360°$, and θ is the angular position of the wire, gives the relationship that

[2] Zangrando, D. and Walker, R.P. A Stretched Wire System for Accurate Integrated Magnetic Field Measurements in Insertion Devices, NIM Volume 376 No.2 p.275 (1996)

$$A_n = \quad nV_{n,\cos} \; / \; \{ \; 2 \; N_t \; r^n \sin (n\Delta\theta/2) \; \}. \qquad (8a)$$

$$B_n = \quad nV_{n,\sin} \; / \; \{ \; 2 \; N_t \; r^n \sin (n\Delta\theta/2) \; \}. \qquad (8b)$$

In these equations, the A's represent the skew component of the field, and the B's represent the normal component of the field.

Integrator data from circular motion of the Litz wire in the mini-undulator gap is shown below. For clarity, only the 2mm, 12mm, and 24mm gaps data is shown. Each data point represents motion of 22.5°. Note that the thumbwheel settings on the integrator were set at $N = N_t * r[mm]$, which is different for each different radius scan. The integrator reading is proportional to the voltage integral divided by N*D, and the voltage integral is proportional to N_t and the wire motion, which is proportional to the radius. Therefore, with the thumbwheel N set at $N = N_t * r[mm]$ the integrator reading was similar for all radius scans.

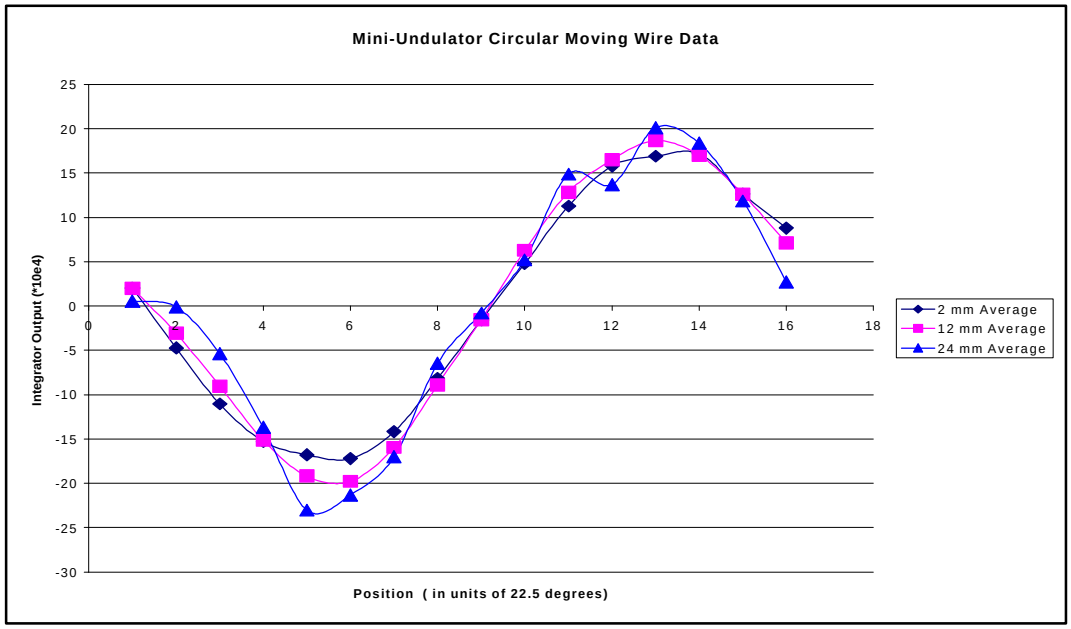

The data displayed in this plot is fit to equation 7, and the tabulated data results for the circular motion of the wire are shown below.

DATA FROM CIRCULAR WIRE MOVEMENT

	2mm	7mm	12mm	17mm	20mm	24mm
NORMAL						
Dipole-Gcm	-458	-476	-481	-484	-481	-479
Quad-G	28.9	34.9	37	33	32.2	31.8
Sext-G/cm	-40.9	15	12	12	12.3	12.3
SKEW						
Dipole-Gcm	49	53	54	53	53	52.6
Quad-G	7.9	8.3	8.1	8.4	8.1	7.9
Sext-G/cm	13.7	-12.2	-8	-8.4	-8.2	-8.7

As expected, the 2mm scan is not very sensitive to the higher moments in the magnetic field, and therefore the values obtained are inconsistent with the larger radii results. The chi-squared fit values were lowest for the 7mm and 12mm data sets. The effect on the multipole values of the number of averages used in the analysis was also examined. The multipole results obtained when 40 points (rather than 20 points) were used for the analysis were similar to the run to run variability of the results. Therefore, 20 points per angular position was determined to be an adequate number of data points. Actually, when only 10 points were used for averaging in, for example, the 7mm scan the dipole, quadrupole, and sextupole varied by only 3Gcm, 3G, and 2G/cm respectively.

Translational Wire Motion

Data was also obtained for purely translational motion of the Litz wire within the gap of the mini-undulator. At the midplane of the magnet gap (i.e. at y=0) , the Litz wire was moved to x positions between –16mm to +16mm about the magnet centerline x=0,y=0 in intervals of 2mm (i.e. at y=0,x=+2mm,-2mm,+4mm,-4mm,+6mm,-6mm,etc). At each of these positions, integrated voltage data was taken as the wire was moved along the x axis (at y=0) from –1mm to + 1mm about the x position. This x motion is sensitive to B_y, the major field component of the magnet. Integrated voltage data was then taken as the wire

was moved from y=+1mm to y=-1mm at each x position. This y motion is sensitive to B_x, the skew field component. The motion was repeated 20 times and the data was collected and averaged, resulting in the following data shown in both tabular and graphic form.

	Translation Data	
X Position (mm)	Y-scan *10 Gcm	X-Scan *10 Gcm
-16	1.875	50.000
-14	2.200	51.075
-12	2.350	51.125
-10	3.175	50.275
-8	2.875	50.325
-6	3.525	50.175
-4	3.550	49.350
-2	3.842	49.250
0	4.825	47.375
2	4.325	47.350
4	3.925	46.950
6	4.975	46.050
8	4.300	44.026
10	4.275	43.350
12	4.000	42.500
14	3.500	41.775
16	3.075	39.500

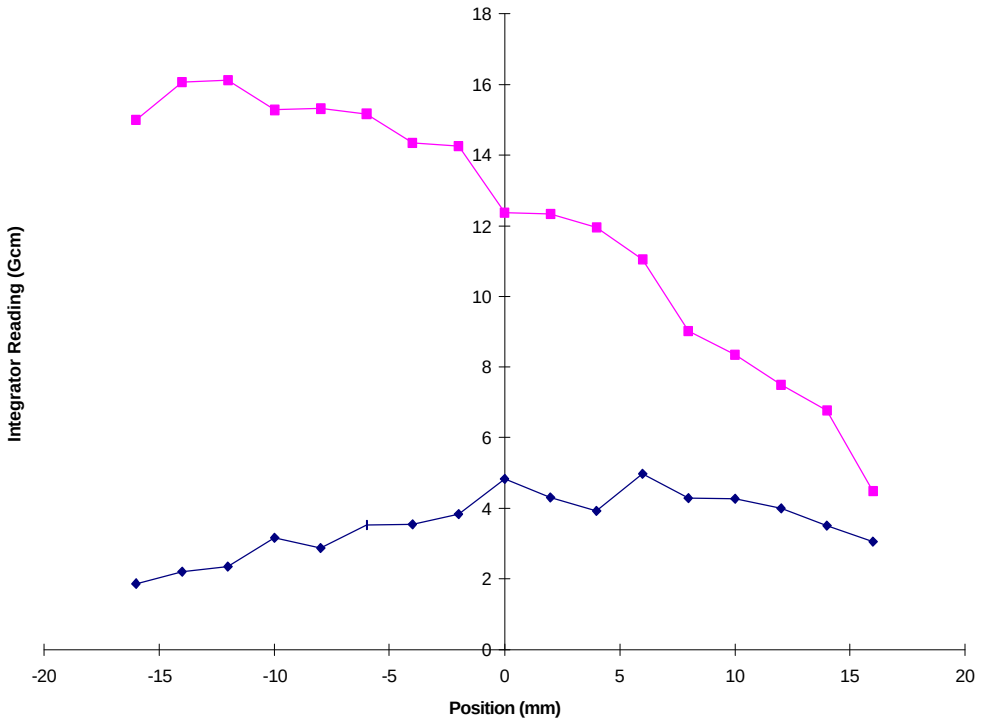

In this plot, the darker diamonds represent the Y scan results (i.e. the B_x field) and the lighter boxes represent the X scan results (i.e. the B_y field). The x-motion results, i.e. the B_y integrals, have been reduced by a constant value of 35 Gcm in the graph to enable both the normal and the skew fields to be seen clearly on the same graph.

This data is analyzed for multipole content by fitting the data to a power series of the form

$$\int V\,dt = B_o + B_1 x + B_2 x^2$$

where Bo is the dipole field, B_1 is the integrated quadrupole, and B_2 is the integrated sextupole. This functional form was applied to the data over various restricted ranges. In order to compare the multipole results from the translational wire motion to the circular wire motion, the range was restricted to +/- 2mm, +/- 8mm, +/- 12mm, and +/-17mm, which includes 3,9,11,and 17 data points respectively.

DATA FROM TRANSLATIONAL WIRE MOVEMENT

	2mm	7mm	12mm	17mm
NORMAL				
Dipole-Gcm	-473	-482	-482	-482
Quad-G	47	37	35	34
Sext-G/cm	231	12	14	12

SKEW				
Dipole-Gcm	48	43	42	42
Quad-G	12	9.4	7.6	5.6
Sext-G/cm	-185	-9.4	-5.9	-6.9

Tabulated data for both circular motion and translational motion of the stretched wire appear below.

Data Summary										
	2mm Circ.	2mm Trans.	7mm Circ.	8mm Trans.	12mm Circ.	12mm Trans.	17mm Circ.	17mm Trans.	20mm Circ.	24mm Circ.
NORMAL										
Dipole-Gcm	-458	-473	-476	-482	-481	-482	-484	-482	-481	-479
Quad-G	28.9	47	34.9	37	37	35	33	34	32.2	31.8
Sext-G/cm	-40.9	231	15	12	12	14	12	12	12.3	12.3
SKEW										
Dipole-Gcm	49	48	53	43	54	42	53	42	53	52.6
Quad-G	7.9	12	8.3	9.4	8.1	7.6	8.4	5.6	8.1	7.9
Sext-G/cm	13.7	-185	-12.2	-9.4	-8	-5.9	-8.4	-6.9	-8.2	-8.7

In order to more easily compare the translational wire motion and the circular wire motion results, all the results of each method were averaged with the exception of the 2mm result. That is, for the circular data, the 7mm,12mm,17mm, and 24mm multipole results were averaged to obtain the values in the table below. The multipole results from the translational data for the 8mm,12mm,and 17mm analysis was also averaged to obtain the values below.

Result Summary for Circular and Translational Data

	Circular Data			**Translational Data**		
	Average	**Std. Dev.**	**SD/AVG**	**Average**	**Std. Dev.**	**SD/AVG**
Gcm	-480.2	2.949576	-0.61424	-482	0	0
G	33.78	2.159167	6.391849	35.33333	1.527525	4.323185
G/cm	12.72	1.283355	10.08927	12.66667	1.154701	9.116057
Gcm	53.12	0.521536	0.981808	42.33333	0.57735	1.36382
G	8.16	0.194936	2.38892	7.533333	1.900877	25.23288
G/cm	-9.1	1.752142	-19.2543	-7.4	1.802776	-24.3618

Clearly, there is excellent agreement between the multipole results obtained from the circular and the translational motion of the integrating wire. Obviously, for wire rotation

at small radii, there is little sensitivity to higher multipoles in the magnetic field. However, both circular and translational motion of the integrating wire at positions of approximately one-third of the magnet half gap was sufficient to determine the multipoles. That is, data at 7mm and 8mm with a magnet gap of 49 mm was sufficient to determine the multipole content of the magnet, while data at only 2mm was clearly not adequate. The translational scans required to obtain the multipoles take about twice as long (i.e. about 2 hours) to complete as the circular motion scans, because in the former case two orthogonal motions are required to determine the normal and skew fields.